Hindawi
Complexity
Volume 2020, Article ID 4939268, 18 pages
https://doi.org/10.1155/2020/4939268

Research Article

A Selection Hyper-Heuristic Algorithm for Multiobjective Dynamic Economic and Environmental Load Dispatch

Le Yang[1], **Dakuo He**[1,2] **and Bo Li**[1]

[1]*College of Information Science and Engineering, Northeastern University, Shenyang 110819, China*
[2]*State Key Laboratory of Integrated Automation for Process Industries, Northeastern University, Shenyang, China*

Correspondence should be addressed to Dakuo He; hedakuo@ise.neu.edu.cn

Received 26 July 2019; Revised 12 September 2019; Accepted 18 December 2019; Published 20 January 2020

Guest Editor: Xiaoqing Bai

Copyright © 2020 Le Yang et al. This is an open access article distributed under the Creative Commons Attribution License, which permits unrestricted use, distribution, and reproduction in any medium, provided the original work is properly cited.

Dynamic economic and environmental load dispatch (DEED) aims to determine the amount of electricity generated from power plants during the planning period to meet load demand while minimizing energy consumption costs and environmental pollution emission indicators subject to the operation requirements. This planning problem is usually expressed using a nonsmooth cost function, taking into account various equality and inequality constraints such as valve-point effects, operational limits, power balance, and ramp rate limits. This paper presents DEED models developed for a system consisting of thermal units, wind power generators, photovoltaic (PV) generators, and energy storage (ES). A selection hyper-heuristic algorithm is proposed to solve the problems. Three heuristic mutation operators formed a low-level operator pool to direct search the solution space of DEED. The high level of SHHA evaluates the performances of the low-level operators and dynamically adjusts the chosen probability of each operator. Simulation experiments were carried out on four systems of different types or sizes. The results verified the effectiveness of the proposed method.

1. Introduction

With the rapid growth of modern industry and global economy, people's demand for electricity in production and life is constantly increasing. Therefore, how to dispatch power production according to the forecasted load demand and improve the generation efficiency of generating units has always been an important research issue in power system operational planning. Traditional economic load dispatch aims to determine the operation status of each unit in a power plant within the planned time and minimize the energy consumption cost while meeting the demand for power load and the operational requirements of generating units. With the gradual attention of human beings to the ecological environment, the harmful substances such as sulfur oxides, nitrogen oxides, and carbon dioxide emitted from fossil fuels to the atmosphere in the combustion process have gradually attracted attention. While reducing energy consumption costs, further reducing environmental pollution emission indicators has become a new requirement for optimizing load dispatch.

For dispatching tasks, energy consumption cost and environmental pollution emissions are two key indicators and minor improvements can bring significant economic and environmental benefits [1]. The optimization of these two indicators is essentially contradictory. Economic and emission load dispatch (EED) is a multiobjective optimization problem that considers these two conflicting indicators at the same time [2]. In addition, because the mathematical expressions of the two indexes are nonconvex and nonsmooth objective functions, it is difficult to solve the optimization problem. The energy crisis caused by the long-term consumption of fossil energy and the global demand for clean energy promotes the development of renewable energy. Wind power, solar power, and plug-in electric vehicles have been widely developed in the last decade and might become the main alternatives in the power system in the near future [3, 4]. But at the same time, the introduction of these renewable energy sources will bring more complex planning and uncertainty to the power grid production [5].

Heuristic optimization algorithms are widely used to solve nonsmooth optimization problems with high

nonlinearity and discontinuity of input and output, such as the economic and environmental dispatch problem, due to their strong global search ability and low requirements for some mathematical properties of the objective function. An improved bacterial foraging algorithm with a parameter automation strategy and crossover operation is proposed to improve computational efficiency and solve the static/dynamic EED [6]. In [7], an improved particle swarm optimization algorithm is applied to EED including solar photovoltaic generation. In [8], a bilevel dynamic economic emission dispatch model is proposed considering wind power integration. Also, robust optimization and a nested solution method are proposed for EED considering wind power uncertainty. A dispatch model combining environmental awareness and risk perception is proposed in [9], and nondominated sorting genetic algorithm-II embedded constraints handling techniques are devised for the problem. In [10], an enhanced multiobjective bee colony optimization algorithm is proposed for solving short-term hydro-thermal-wind complementary scheduling considering the uncertainty of wind power. In [2], a dynamic economic emission dispatch (DEED) incorporating renewable energy and energy storage is formulated and an adaptive robust method is proposed to solve the problem.

There are many differences in EED models that have been solved in the existing research. Some scholars focus on the dynamic economic emission dispatch (DEED) problems which consider only thermal generation, single-objective DEED with renewable energy generation (REG), and the multiobjective static DEED with REG. This paper formulates a DEED model including thermal generation, wind energy generation, solar photovoltaic (PV) generation, and energy storage (ES). A selection hyper-heuristic algorithm is proposed to solve the Pareto optimal solution of the problem. Three operators formed a low-level operator pool to directly search the solution space. The high-level structure is responsible for managing low-level operators. The operators are evaluated and ranked by analyzing the results of the nondominated solutions. Then, the chosen probability of each low-level operator is determined by the selection mechanism, which is provided for the next call. The effectiveness of the optimization strategy is validated through a series of simulations. The results are compared with those of existing state-of-the-art optimization techniques.

The rest of this paper is organized as follows. Section 2 presents the DEED mathematical model. The application of the proposed hyper-heuristic method is described in Section 3. To illustrate its effectiveness, the proposed method was tested on a series of systems in Section 4. Conclusions and future research are discussed in Section 5.

2. Problem Formulation

In this section, we will discuss the mathematical model of the DEED problem, which is used to distribute the output power of all generators economically and environmentally during the dispatching period and satisfies a series of equality and inequality constraints.

2.1. Objective Function. Compared with the static EED, which is scheduled at a certain hour, DEED adopts dynamic scheduling for a load cycle of 24 hours. Consider a power system with N_G thermal power generators, N_W wind power generators, and N_{PV} PV generators over time intervals. The basic objective function of the DEED problem can be formulated as the following optimal function:

$$\begin{aligned}\min F &= \sum_{t=1}^{N_T}\left(\sum_{i=1}^{N_G} F_i\left(P_{i,t}\right) + \sum_{i=1}^{N_w} F_i\left(w_{i,t}\right) + \sum_{i=1}^{N_{PV}} F_i\left(\mathrm{PV}_{i,t}\right)\right),\\ \min E &= \alpha_i P_{i,t}^2 + \beta_i P_{i,t} + \gamma_i + \eta_i \exp\left(\delta_i P_{i,t}\right),\end{aligned} \tag{1}$$

where i and t are the number of generator and time interval, respectively. F denotes the total fuel costs over the dispatch period. $F_i(P_{i,t})$, $F_i(w_{i,t})$, and $F_i(\mathrm{PV}_{i,t})$ are cost functions of the thermal power generator, wind power generator, and solar power generator, respectively. N_T is the time horizon. $P_{i,t}$, $W_{i,t}$, and $\mathrm{PV}_{i,t}$ are the power output of thermal power generator, wind power generator, and PV generator, respectively. α_i, β_i, γ_i, η_i, and δ_i are environmental cost coefficients.

When the valve-point effect (VPE) is considered, the total fuel costs of thermal power generators can be written as follows:

$$F_i\left(P_{i,t}\right) = a_i P_{i,t}^2 + b_i P_{i,t} + c_i + \left|e_i \sin\left(f_i\left(P_i^{\min} - P_{i,t}\right)\right)\right|, \tag{2}$$

where $P_{i,\min}$ is the minimum power outputs of generator i. a_i, b_i, and c_i are the fuel cost coefficients of generator i. e_i and f_i are the coefficients of generator i reflecting the valve-point effects. Valve-point effect is the phenomenon of rapid increase consumption caused by valve drawing effects during start-up of thermal power generators.

The total economic costs of wind power generators can be written as follows:

$$\begin{aligned}F_i\left(w_{i,t}\right) &= c_{w,i}\left(w_{i,t}\right) + c_{p,w,i}\left(W_{it,\mathrm{av}} - w_{i,t}\right) + c_{r,w,i}\left(w_{i,t} - W_{it,\mathrm{av}}\right),\\ c_{wi}\left(w_{i,t}\right) &= d_i w_{i,t},\\ c_{p,wi} &= k_{p,i}\left(W_{ij,\mathrm{av}} - w_{i,t}\right) = k_{p,i}\int_{w_i}^{w_{ri}}\left(w - w_{i,t}\right) f_w(w)\mathrm{d}w,\\ c_{r,wi} &= k_{r,i}\left(w_{i,t} - W_{ij,\mathrm{av}}\right) = k_{r,i}\int_{0}^{w_i}\left(w_{i,t} - w\right) f_w(w)\mathrm{d}w,\end{aligned} \tag{3}$$

where $w_{i,t}$ and $W_{it,av}$ are the schedule and actual power of wind generator i at time interval t. $c_{w,i}$ denotes the cost function of generator i (payment to wind farm operators for actual use of wind power), which can be calculated by the cost coefficients and the wind probability density function. d_i is the direct cost coefficient of generator i. $c_{p,w,i}$ denotes the penalty cost function for not using all available power of generator i, which has a linear correlation with the difference between available power and actual power. $k_{p,i}$ is the underestimating penalty cost coefficient. $f_w(w)$ is the probability distribution function of wind power. $c_{r,w,i}$ denotes the reserve costs associated with wind power

uncertainty (penalties for estimating available wind power). w_{ri} is the rated power of generator i, and $k_{r,i}$ is the reserve cost coefficient.

The total economic costs of solar power generators can be written as follows:

$$\begin{aligned} F_i(w_{i,t}) &= c_{pvi}(\mathrm{pv}_{i,t}) + c_{p,pvi}(\mathrm{PV}_{it,\mathrm{av}} - \mathrm{pv}_{i,t}) \\ &\quad + c_{r,pvi}(\mathrm{pv}_{i,t} - \mathrm{PV}_{it,\mathrm{av}}), \\ c_{pvi}(\mathrm{pv}_{i,t}) &= h_i f_{\mathrm{pv}}(\mathrm{pv})\mathrm{pv}_{i,t}, \\ c_{p,pvi} &= k_{p,pvi}(\mathrm{PV}_{ij,\mathrm{av}} - \mathrm{pv}_{i,t}) \\ &= k_{p,pvi}\int_{\mathrm{pv}_i}^{\mathrm{pv}(k_{\max})}(\mathrm{pv} - \mathrm{pv}_{i,t}) f_{pv}(\mathrm{pv})\mathrm{d}pv, \\ c_{r,pvi} &= k_{r,pvi}(\mathrm{pv}_{i,t} - \mathrm{PV}_{ij,\mathrm{av}}) \\ &= e_{r,pvi}\int_0^{\mathrm{pv}_{ri}}(\mathrm{pv}_{i,t} - \mathrm{pv}) f_{pv}(\mathrm{pv})\mathrm{d}pv, \end{aligned} \tag{4}$$

where $\mathrm{pv}_{i,t}$ and $\mathrm{PV}_{it,\mathrm{av}}$ are the schedule and actual power of solar generator i at time interval t. c_{pvi} denotes the weighted cost of generator i based on solar irradiance, which can be calculated by the cost coefficients and the solar probability density function. $c_{p,pvi}$ and $c_{r,pvi}$ are the penalty cost function for not using all available power of generator and the reserve costs associated with power uncertainty, respectively. h_i is the operating cost coefficient of solar power operator. pv_{ri} is the rated power of generator i, and $\mathrm{pv}(k_{\max})$ is the upper limit of output of the corresponding operator. $k_{p,pvi}$ and $k_{r,pvi}$ are the underestimating penalty cost coefficient and the reserve cost coefficient, respectively. $f_{\mathrm{pv}}(\mathrm{pv})$ is the probability distribution function of solar power.

2.2. Constraints

(1) Real Power Balance Constrains

In order to ensure the safe and stable operation of generators, each generator needs to run in a specified power range:

$$\begin{aligned} \sum_{i=1}^{N_G} P_{i,t} + \sum_{i=1}^{N_w} w_{i,t} + \sum_{i=1}^{N_{\mathrm{PV}}} \mathrm{PV}_{i,t} + \sum_{i=1}^{N_{\mathrm{ES}}} \mathrm{ES}_{i,t} &= P_{D,t} + P_{L,t}, \quad t \in N_T, \\ P_{L,t} = \sum_{i=1}^{N_T}\sum_{j=1}^{N_T} P_{i,t}B_{ij}P_{j,t} + \sum_{i=1}^{N_T} B_{0i}P_{i,t} + B_{00}, &\quad t \in N_T, \end{aligned} \tag{5}$$

where $P_{i,\min}$ and $P_{i,\max}$ are the minimum and maximum power outputs of thermal generator i, respectively. $\mathrm{ES}_{ch,i}$ and $\mathrm{ES}_{\mathrm{dis},i}$ denote the charge and discharge power of the ith ES unit. $\mathrm{ES}_{i,\mathrm{cap}}$ is the power capacity of ith ES unit.

(2) Power Operating Constrains

In order to ensure the safe and stable operation of generators, each generator needs to run in a specified power range:

$$\begin{aligned} P_{i,\min} \le P_{i,t} \le P_{i,\max}, &\quad i \in N_G\, t \in N_T, \\ 0 \le w_{i,t} \le w_{ri}, &\quad i \in N_w\, t \in N_T, \\ 0 \le \mathrm{pv}_{i,t} \le \mathrm{pv}(k_{\max}), &\quad i \in N_{\mathrm{pv}}\, t \in N_T, \\ -\mathrm{ES}_{i,\mathrm{cap}} \le \mathrm{ES}_{ch,i} \le 0, &\quad i \in N_{\mathrm{ES}}, \\ 0 \le \mathrm{ES}_{\mathrm{dis},i} \le \mathrm{ES}_{i,\mathrm{cap}}, &\quad i \in N_{\mathrm{ES}}, \end{aligned} \tag{6}$$

where $P_{i,\min}$ and $P_{i,\max}$ are the minimum and maximum power outputs of thermal generator i, respectively. $\mathrm{ES}_{ch,i}$ and $\mathrm{ES}_{\mathrm{dis},i}$ denote the charge and discharge power of the ith ES unit. $\mathrm{ES}_{i,\mathrm{cap}}$ is the power capacity of the ith ES unit.

(3) Generator Ramp Rate Constrains

The power output of the generators should not fluctuate too much during the interval time interval. Ramp rate constraints are used to restrict the adjusting range of the generator power:

$$P_{i,t-1} - \mathrm{DR}_i \le P_{i,t} \le P_{i,t-1} + \mathrm{UR}_i, \quad i \in N_G, \tag{7}$$

where UR_i and DR_i are the ramp-up and ramp-down rate constraints of generator i, respectively.

(4) Spinning Reserve Requirements

Spinning reserve requirements (SRRs) refer to the readily available capacity, which can compensate for the generation gap caused by generator faults or power fluctuation in a short time. SRR constraints are frequently applied in the unit commitment problem and economic dispatch problem [11–13]. It can be employed to provide the operating reserves to balance the influence brought by the renewables uncertainty and forecast error [14].

$$\begin{aligned} &\sum_{i=1}^{N_G} P_{i,\max} - (P_{D,t} + P_{L,t}) \ge \mathrm{SR}_t, \quad t \in N_T, \\ &\sum_{i=1}^{N_G} (\min(P_{i,\max} - P_{i,t}, \mathrm{UR}_i)) \ge \mathrm{SR}_t, \quad t \in N_T, \\ &\sum_{i=1}^{N_G} \left(\min\left(P_{i,\max} - P_{i,t}, \frac{\mathrm{UR}_i}{6}\right)\right) \ge \mathrm{SR}'_t, \quad t \in N_T, \end{aligned} \tag{8}$$

where SR_t and SR'_t are the spinning reserves for the one-hour and 10-minute compensation time.

(5) Energy Storage SOC Constraints

The state of charge (SOC) denotes an ES's real-time power state, which is the variable that actually operates in the scheduling process. It is calculated according to the state at the previous time interval:

$$\mathrm{SOC}_{\min} \le \mathrm{SOC}_{i,t} \le \mathrm{SOC}_{\max}, \tag{9}$$

where $\mathrm{SOC}_{i,t}$ is the SOC of the ith ES at time interval t which lies between 0 and 1. $\mathrm{SOC}_{\min}$ and $\mathrm{SOC}_{\min}$ are the minimum and maximum limits of SOC, respectively.

3. Multiobjective Selection Hyper-Heuristic Algorithm

In this paper, a selection hyper-heuristic algorithm is used to solve the Pareto optimal solution of the DEED problem. The method consists of two levels, and the low-level structure contains an algorithm pool, which is composed of three heuristic operators to directly search the solution space. In the management of the high-level structure, the low-level operators are evaluated and ranked by calculating the results of nondominated solutions. Then, the chosen probability of each low-level operator is calculated through the selection mechanism, which is provided for the next call.

3.1. The Framework of Selection Hyper-Heuristic Algorithm. Hyper-heuristic algorithms are widely used in the field of automatic algorithm design [15]. Hyper-heuristics can be defined as "automated methods for selecting or generating heuristics to solve hard computing search problems." [16] This is different from most implementations of meta-heuristic methods that operate directly on solution spaces. It was originally used in 1997 to describe a protocol that combines several AI methods in the context of automatic theorem proving. The proposed multiobjective selection hyper-heuristic algorithm is shown in Figure 1. The low-level operator pool consists of three heuristic operators, and the high level of the proposed algorithm consists of an evaluation strategy and a selection mechanism.

The low-level operator pool plays an important role in searching the problem space effectively. A mutation operator pool composed of three different mutation operators is built in this section. These operators will be implemented under the guidance of an adaptive selection mechanism at different stages of the search. The operators are as follows:

$H1$: GA/derived from NSGA-II

$$c_k = p_k + \left(p_k^u - p_k^l\right)\delta_k. \tag{10}$$

$H2$: DE/rand/2

$$v_i^G = x_{r1}^G + F\left(x_{r2}^G - x_{r3}^G\right) + F\left(x_{r4}^G - x_{r5}^G\right). \tag{11}$$

$H3$: DE/current-to-best/1 derived from PSO

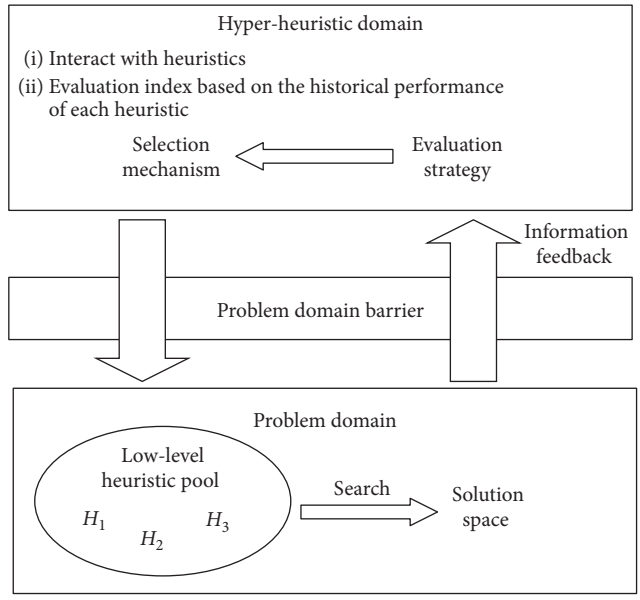

Figure 1: Framework of the proposed selection hyper-heuristic algorithm.

$$v_i^G = G_r x_{\text{best}}^G + (1 - G_r)x_i^G + F\left(x_{r1}^G - x_{r2}^G\right), \tag{12}$$

where c_k is the offspring and p_k is the parent with p_k^u being the upper bound on the parent component, p_k^u is the lower bound, and δ_k is small variation which is calculated from a polynomial distribution [17].

Instead of operating directly on a solution space, the high level of the hyper-heuristics evaluates and grades the historical performance of the low-level operators during a given stage. A selection mechanism is devised to manage the calls of the low-level operators at different stages in the searching process. The underlying assumption is that each low-level operator has different performance in different regions of search space or at different stages of the whole searching process [15]. In fact, due to the function landscapes of the problems and the characteristics of the operators, it is difficult for the operator to keep stable optimization capability in different regions of the whole search area. It is common that some operators perform well in the early stage of iteration, but lack optimization capability in the later stage. Here, we introduce a sliding time window (STW) to dynamically evaluate the historical performance of the low-level operators. The length of the STW is much smaller than the maximum number of iteration. The uniformity of the nondominated solution and the dominated relationship between parent and offspring individuals are used as the evaluation indexes.

The specific steps of the evaluation and selection mechanism are as follows:

Step 1 (evaluation): compute the spatial measure (uniformity) of nondominated solutions, sp.

Step 2: calculate the number of the parent dominated by the offspring $\mathrm{dom}_{o,p}$, and the number of the parent and the offspring does not dominate each other, dom.

Step 3: calculate FIR score:

$$\mathrm{FIR} = 1 * \mathrm{dom}_{o,p} + 0.5 * \mathrm{dom}. \tag{13}$$

Step 4: update the sliding window time, SWT(FIR, sp), and the historical information, history(FIR, sp).

Step 5 (selection): collect the number of call frequency of each operator, $Cn_{\mathrm{total}} = \mathrm{sum}(Cn)$.

Step 6: determine the chosen probability based on historical information:

$$Pn = \mathrm{FIR} + \frac{C_1 * Cn}{Cn_{\mathrm{total}}} + C_2 * sp + C_3 * \mathrm{history}(\mathrm{FIR}) + C_4 * \mathrm{history}(sp). \tag{14}$$

Step 7: select the low-level operator using the roulette method.

3.2. Elitist Nondominated Sorting Mechanism. In different periods of iteration, the crowding distance between individuals is used as an index to guide the selection of parent individuals. In the early stage of iteration, the combination of nondominated sorting and crowding distance is used to select individuals. Firstly, the nondominated sorting of solutions is performed to obtain different Pareto frontiers of solutions. Then, the individuals are sorted in descending order of crowding distance in each Pareto frontier. Finally, 75% of the larger crowding distance in each Pareto frontier is selected as the paternal individuals until the total number of parent individuals is satisfied. At the later stage of the iteration, the population converges gradually and the density of solutions in the population is high. This paper combines nondominated sorting, crowding distance, and hypercube grid to select parent individuals. Individuals will be screened in two ways. One is nondominated sorting. The other is a combination of nondominated sorting, crowding distance, and hypercube grid. A parameter λ is introduced to decide which way to choose. First, individuals are screened using the same steps as in the early stage. Then, the selected individuals are put into the grid, and the grid with larger individual density is screened. In each selected grid, some individuals are randomly selected for deletion to guarantee the uniform distribution of individuals. By introducing crowding distance and hypercube grid, not only the diversity of the population is guaranteed but also the individuals are evenly distributed in the solution space. This helps to improve the diversity of the algorithm and maintain its search capability (Algorithm 1).

3.3. Constraint Handling. DEED involves a number of equality and inequality constraints. We cannot guarantee every generated solution will satisfy all constraints, especially real power balance and ramp rate constraints. Penalty-based methods are the most commonly used methods to deal with these complex constraints, but it has some shortcomings in the calculation efficiency. Furthermore, how to determine the punishment degree is also a challenge. In this section, we devised a heuristic process to deal with the constraints. Compared with [18], our method can avoid the situation that the output power of the adjacent hour violates the power balance constraints, especially at the later stage of the adjustment process. Handling of the SRRs in this chapter is referenced from Ref. [19].

Step 1: randomly select an hour $t \in N_T$.

Step 2: calculate the corresponding feasible region of the adjustable output:

$$P_{i,t}^{\min} = \begin{cases} \max\left(P_{i,\min}, P_{i,t+1} - \mathrm{UR}_i\right), & t = 1, \\ \max\left(P_{i,\min}, P_{i,t-1} - \mathrm{DR}_i\right), & t = N_T, \\ \max\left(\max\left(P_{i,\min}, P_{i,t-1} - \mathrm{DR}_i\right), P_{i,t+1} - \mathrm{UR}_i\right), & 1 < t < N_T, \end{cases} \tag{15}$$

$$P_{i,t}^{\max} = \begin{cases} \min\left(P_{i,\max}, P_{i,t+1} + \mathrm{DR}_i\right), & t = 1, \\ \min\left(P_{i,\max}, P_{i,t-1} + \mathrm{UR}_i\right), & t = N_T, \\ \min\left(\min\left(P_{i,\max}, P_{i,t+1} + \mathrm{DR}_i\right), P_{i,t-1} + \mathrm{UR}_i\right), & 1 < t < N_T. \end{cases} \tag{16}$$

Step 3: adjust the output of each generator at the current hour to satisfy (15) and (16) using (17):

$$P_{i,t} = \begin{cases} P_{i,t}^{\min}, P_{i,t} < P_{i,t}^{\min}, \\ P_{i,t}, P_{i,t}^{\min} \le P_{i,t} \le P_{i,t}^{\max}, \\ P_{i,t}^{\max}, P_{i,t} > P_{i,t}^{\max}. \end{cases} \tag{17}$$

Step 4: tackle the SRR constraints: check if SRRs is satisfied and then go to Step 5; otherwise, calculate the violation of SRRs $\Delta_{\mathrm{SRRs},t}$ and set $t = t - 1$. Subtract $\Delta_{\mathrm{SRRs},t}$ from $P_{i,t}^{\max}$ which are equal to their upper limits. Then, generate a new feasible individual at hour $t - 1$. Calculate $\Delta_{\mathrm{SRRs},t-1}$ and repeat the adjust process until the SRR constraints are satisfied at an hour.

Step 5: tackle the demand-supply constraint by the following steps:

(1) Calculate the system transmission loss using (5).

(2) Calculate the difference between the power demand and the power grid output:

$$\mathrm{Dif} = P_{D,t} + P_{L,t} - \left(\sum_{i=1}^{N_G} P_{i,t} + \sum_{i=1}^{N_w} w_{i,t} + \sum_{i=1}^{N_{\mathrm{PV}}} \mathrm{PV}_{i,t} + \sum_{i=1}^{N_{\mathrm{ES}}} \mathrm{ES}_{i,t}\right). \tag{18}$$

Check if $\mathrm{Dif} \le \varepsilon_0$ and then go to Step 2 with the next randomly selected hour; otherwise, go to the next step. Here, ε_0 is a tolerance variable which decreases from early stages of the evolutionary process and is decreased gradually to a small value [20].

(3) Generate a random sequence $R = [r_1, r_2, \ldots, r_{N_G}]$. Select $P_{r,t}$ as the first slack generator and adjust its power as

Input: τ, λ, iterMax
Output: Screened individuals
(1) **initialize**: Set $\tau = 0.5$
(2) **if** iter $< \tau *$ iterMax **then**
(3) Screen using a combination of nondominated sorting and crowding distance
(4) **else**
(5) $\lambda = \tau + (1 - \tau) *$ (iter/iterMax)
(6) **if** rand $< \lambda$ **then**
(7) Screen using the nondominated sorting
(8) **else**
(9) Screen using a combination of nondominated sorting and crowding distance and hypercube grid
(10) **end if**
(11) **end if**

Algorithm 1: Elitist nondominated sorting strategy.

$$P_{r,t} = \begin{cases} P_{r,t} + \text{Dif} * \Delta, & \text{if Dif} > 0, \\ P_{r,t} - \text{Dif} * \Delta, & \text{if Dif} < 0. \end{cases} \quad (19)$$

(4) Adjust $P_{r,t}$ using (17) to satisfy the feasible region limit. Update Dif and select the next slack generator in turn according to R. Δ is a random value which lies between [0.2, 1].

Step 6: repeat the previous steps until a feasible solution is found.

3.4. Selection Hyper-Heuristic Algorithm for DEED. The detailed procedure of the proposed method for DEED is presented as follows:

Step 1: initialize the setting parameters of the algorithm, such as population size, the maximum number of iteration, number of objective, and parameters of low-level operators.

Step 2: generate the initial population, perform the nondominated sorting, and calculate the crowding distance.

Step 3: select individuals to build up the parent population using the tournament selection, and then generate the initial offspring population by calling the low-level operators.

Step 4: memorize the current iteration number and start the evolution process.

Step 5: combine the parent population and the offspring population, conduct the nondominated sorting strategy, and update the crowding distance.

Step 6: select the parent individuals using the proposed nondominated sorting strategy mentioned in the previous section, and then generate the offspring individuals.

Step 7: grade and rank the low-level operators using the evaluation method presented in the previous section.

Step 8: choose the low-level operator using the selection mechanism presented in the previous section.

Table 1: Related parameters for case study.

Population size	150
Maximum iteration	250
Parameters for ES	$\text{SOC}_{\min} = 0.2$, $\text{SOC}_{\max} = 1$, $E_{\max} = 300$ WM, $\Delta t = 0.92$
Parameters for high level	SWT = 15, $C_1 = C_2 = 0.4$, $C_3 = C_4 = 0.1$
Parameters for low level	$F_{\min} = 0.2$, $F_{\max} = 0.8$, $G_{r,\min} = 0.3$, $G_{r,\max} = 0.8$, $F = \text{rand}(F_{\min}, F_{\max})$
Operators	$G_r = G_{r,\min} + (G_{r,\max} - G_{r,\min}) * \exp(-2 * (\text{iterMax} - \text{iter}))/\text{iter}$

Step 9: memorize the optimal solution and check whether the current iteration is greater than the maximum iteration number. If not, continue the cycle; otherwise, output the global optima solution.

The flowchart of the proposed method is presented as follows.

4. Results and Discussion

For the experimental study, four test cases are studied to evaluate the performance of the proposed algorithm. The scheduling time N_T of all cases is selected as one day with 24 hours, and the valve-point effect and the ramp rate constraints are taken into account. Case 1 and Case 2 are classic DEEDs with 5 thermal units and 10 thermal units without considering wind and PV generation, respectively. We use these two cases to verify the effectiveness of our proposed method by comparing them with the existing algorithms. Case 3 comes from an IEEE 57 bus system; three PV and two wind generators are incorporated into this system. Case 4 considers the ES unit on the basis of Case 3. We use this case to study the impact of ES on the system operation and its role in peak shaving and valley filling in the power supply.

Wind power output depends on wind speed, type of wind turbine, and parameters of its power performance curve. Wind speed is a random variable that needs to be

Table 2: Optimal results for Case 1 (optimal cost).

H	P_1	P_2	P_3	P_4	P_5	P_L	E_c (\$)	E_m (lb)
1	20.24	98.62	30.00	125.04	139.91	3.82	1250.56	546.67
2	10.00	97.91	66.84	124.79	139.63	4.13	1425.15	534.83
3	10.00	98.41	106.83	124.89	139.76	4.78	1392.40	558.72
4	25.80	98.53	112.78	124.91	173.81	5.91	1732.18	682.12
5	19.31	98.51	112.68	124.84	209.36	6.63	1721.24	845.55
6	49.31	99.20	112.71	124.94	229.59	7.85	1785.23	977.50
7	68.80	98.43	112.66	124.89	229.52	8.31	1799.13	1002.70
8	74.99	98.51	112.67	147.37	229.53	9.05	1980.10	1053.38
9	62.16	98.45	112.65	197.37	229.53	10.12	2046.26	1152.18
10	63.96	98.57	112.71	209.81	229.51	10.56	1997.11	1194.64
11	74.51	98.50	112.67	209.81	235.47	11.04	2050.82	1251.31
12	74.98	98.52	112.67	180.08	285.45	11.77	2412.73	1570.83
13	73.53	98.54	112.67	130.08	300.00	10.77	2150.49	1624.19
14	64.27	98.51	112.67	124.90	300.00	10.37	2106.36	1599.32
15	34.27	98.52	112.68	124.89	292.92	9.34	2047.42	1486.71
16	10.00	96.91	112.65	124.90	242.92	7.28	1711.12	1046.39
17	10.00	92.79	107.59	124.88	229.52	6.71	1618.85	943.40
18	35.87	98.57	113.09	138.69	229.56	7.86	1854.71	987.96
19	34.05	98.48	112.50	188.67	229.52	9.14	1998.32	1098.70
20	64.05	98.54	112.67	209.74	229.51	10.56	1996.98	1194.40
21	39.29	98.59	112.68	209.79	229.53	9.90	1944.92	1166.62
22	10.00	96.86	112.61	209.82	183.54	7.91	1874.26	920.06
23	10.00	66.86	106.92	209.74	139.59	6.01	1651.80	693.75
24	10.02	36.86	71.38	209.82	139.76	4.80	1584.27	641.47
Total						194.61	44132	24773

predicted and has uncertainty. The previous study has proved that the wind speed at a given location closely follows a Weibull distribution over time [21]. The output power of wind turbines can be predicted by the PDF of wind speed and the wind speed-power curve. The detailed calculation steps and parameters can be found in [22]. The output power of the PV can be calculated by predicting solar radiation. However, the solar radiation reaching the Earth's surface depends upon the climatic conditions of a location [23]. The calculation steps of power of PV are detailed in [24]. The parameters used for solving DEED in this study are shown in Table 1. For each case, 20 independent trials were conducted to compare the solution quality and convergence characteristics. All experiments were executed in the MATLAB 2016a computational environment on a Pentium-core 3.2 GHz personal computer with 8 GB of RAM.

4.1. Case Study

4.1.1. Case 1: Classic 5-Generator System. This test system consists of five thermal generators with considering the transmission loss. The generating system data and B coefficients to compute transmission line losses are adapted from [25]. The best cost and emission solutions are given in Tables 2 and 3, respectively. The compromise solution considering economic and emission is presented in Table 4. H represents the dispatch hour, and P_i denotes the output power allocated to the ith thermal generator. P_L is the transmission line losses. E_c and E_m are the fuel cost and emission, respectively. The optimal cost and emission solutions are 44132 \$/day and 17852 lb/day, respectively. The minimum cost and emission of the best compromise solution are 47503 \$/day and 18066 lb/day, respectively. Table 5 gives the comparison among different methods, such as SA, MSL, EP, PS, PSO, MODE, and AGB-MOCDE. It is obvious that the proposed method can obtain solutions with lower total economic costs and emission than other reported methods.

4.1.2. Case 2: Classic 10-Generator System. This case consists of ten thermal generators with considering the transmission loss. The generating system data and B coefficients can be obtained in [26]. The best cost and emission solutions are given in Tables 6 and 7, respectively. The compromise solution considering economic and emission is presented in Table 8. The optimal cost and emission solutions are 2471526 \$/day and 291988 lb/day, respectively. The minimum cost and emission of the best compromise solution are 2514885 \$/day and 299585 lb/day, respectively. The simulation results of the proposed methods are compared in Table 5 with NSGA-II, EP, PSO, SQP, HMO-DE-PSO, RCGA, MADM, IBFA, and MODE. It is obvious that the proposed method can obtain solutions with lower total economic costs and emission than other reported methods.

To test the convergence characteristics of the proposed method, we conducted a comparison experiment in the same experiment situation for Case 2. Two typical methods, NSGA-II and MODE, are used to compare with SHHA. 20 independent trials were conducted to compare the convergence characteristics. Figure 1 shows the convergence

Table 3: Optimal results for Case 1 (optimal emission).

T_H	P_1	P_2	P_3	P_4	P_5	P_L	E_c ($)	E_m (lb)
1	54.70	58.19	116.56	110.45	73.53	3.45	1725.14	352.44
2	58.08	62.25	121.85	118.38	78.31	3.89	1780.62	385.95
3	63.38	69.20	129.91	129.92	87.22	4.64	1911.96	446.63
4	71.45	78.37	141.62	145.50	98.84	5.79	2133.65	544.63
5	75.00	83.35	147.28	153.69	105.10	6.43	2202.49	601.19
6	75.00	93.80	158.96	170.11	117.76	7.65	2243.16	715.00
7	75.00	97.29	163.13	175.88	122.81	8.12	2224.83	760.33
8	75.00	103.27	169.13	185.29	130.17	8.88	2220.35	835.62
9	75.00	111.46	175.00	197.50	140.94	9.91	2208.04	941.41
10	75.00	115.23	175.00	203.39	145.70	10.34	2255.86	985.83
11	75.00	119.96	175.00	209.65	151.21	10.83	2309.83	1039.14
12	75.00	125.00	175.00	217.44	159.02	11.47	2471.19	1109.73
13	75.00	115.47	175.00	203.26	145.60	10.34	2257.14	985.83
14	75.00	111.45	175.00	197.75	140.71	9.91	2204.96	941.40
15	75.00	103.10	169.04	185.62	130.10	8.88	2218.84	835.62
16	75.00	87.67	152.34	160.92	111.02	6.95	2237.17	649.10
17	75.00	83.06	147.41	154.03	104.91	6.43	2205.58	601.19
18	75.00	93.38	158.92	170.34	118.01	7.65	2244.08	714.99
19	75.00	103.32	169.05	185.41	130.09	8.88	2220.96	835.62
20	75.00	115.41	175.00	203.31	145.61	10.34	2256.62	985.83
21	75.00	108.69	174.99	193.68	137.25	9.62	2201.34	910.92
22	75.00	92.86	158.27	169.19	117.25	7.58	2244.93	707.67
23	70.84	77.94	141.08	144.61	98.25	5.73	2124.57	538.84
24	61.83	67.19	127.45	126.28	84.65	4.41	1849.31	427.50
Total						188.13	51953	17852

Table 4: Optimal compromise results for Case 1.

H	P_1	P_2	P_3	P_4	P_5	P_L	E_c ($)	E_m (lb)
1	60.68	65.18	112.89	124.70	50.07	3.51	1461.20	362.60
2	63.25	78.87	112.39	125.02	59.42	3.95	1538.25	396.97
3	72.17	81.73	117.52	124.93	83.33	4.67	1738.45	453.15
4	75.00	90.54	127.86	126.08	116.32	5.80	1838.91	557.48
5	74.99	97.06	132.76	126.87	132.76	6.43	1798.62	624.45
6	74.99	98.37	160.99	141.66	139.61	7.62	2000.13	730.30
7	75.00	98.21	160.02	169.65	131.22	8.11	2178.50	761.97
8	75.00	98.51	163.85	187.80	137.71	8.87	2144.33	837.33
9	75.00	100.43	174.97	209.76	139.77	9.91	2062.54	945.48
10	75.00	114.67	175.00	209.79	139.90	10.36	2172.01	986.93
11	75.00	125.00	175.00	210.00	145.86	10.86	2292.06	1040.11
12	75.00	125.00	175.00	214.67	161.79	11.46	2467.32	1109.97
13	75.00	114.34	174.98	209.80	140.24	10.36	2172.79	986.88
14	75.00	100.26	175.00	209.82	139.84	9.91	2061.54	945.54
15	75.00	98.40	165.56	184.52	139.39	8.86	2143.03	837.42
16	75.00	98.43	145.18	134.52	133.82	6.94	1926.89	665.95
17	74.81	97.49	134.45	125.36	132.33	6.43	1797.18	624.51
18	74.98	98.53	162.28	140.16	139.67	7.62	1988.62	731.37
19	75.00	98.48	166.20	185.63	137.55	8.86	2149.55	836.91
20	75.00	114.74	175.00	209.85	139.76	10.36	2171.44	986.96
21	74.39	98.34	174.96	202.34	139.58	9.61	2080.14	914.34
22	74.99	98.50	146.73	152.80	139.54	7.56	2039.88	719.77
23	74.91	98.19	114.13	125.80	119.74	5.77	1691.22	564.86
24	67.58	92.99	112.66	124.32	69.93	4.49	1588.60	444.58
Total						188.35	47503	18066

comparison when aiming to optimize the fuel cost. The figure indicates that the SHHA converges faster than other methods. In addition, the statistical results of the 20 trails are given in Table 9. It can be seen that the SHHA outperforms the other methods regardless of minimum cost, average cost, and maximum cost. The SHHA has a lower standard deviation which also shows a better robustness (Figures 2 and 3).

Table 5: Comparison of the results for Case 1 and Case 2.

Method	Minimum cost		Minimum emission		Compromise result		Computational time (min)
	E_c ($)	E_m ($)	E_c ($)	E_m ($)	E_c ($)	E_m (lb)	
Case 1							
SA [25]	47356	—	—	—	—	—	NA
MSL [27]	49216.81	—	—	—	—	—	NA
EP [28]	46777	—	—	17966	48628	21154	NA
PS [28]	46530	—	—	18192	47911	18927	4.91
PSO [29]	47852	22405	—	—	50893	20163	NA
MODE [30]	46934	18194	48841	18008	47714	18084	15
MOHDE-SAT [31]	46478	18208	50684	17884	48214	18011	14.55
AGB-MOCDE [25]	46230	18295	49866	17927	47589	18075	NA
This paper	44711	22000	51953	17852	47503	18066	9.33
Case 2							
NSGA-II [26]	—	—	—	—	2522600	309940	20.11
EP [32]	2585000	—	—	—	—	—	NA
PSO [14]	2572000	—	—	—	—	—	NA
SQP [14]	2519000	343400	2628000	308000	2535000	329300	
MOHDE-SAT [31]	2,508,195	334100	2606000	295900	2525000	303900	16.17
RCGA [26]	2516800	317400	2656300	304120	2525100	312460	18
MADM [33]	—	—	—	—	2590500	291960	15
IBFA [6]	2481733	327501	2614341	295833	2517116	299036	5.2
MODE [30]	2512327	301130	2543560	296387	2525841	298344	16.76
This paper	2471526	332300	2598103	291988	2517013	299005	10.85

NA denotes that the value was not available in the literature.

Table 6: Optimal results for Case 2 (optimal cost).

H	P_1	P_2	P_3	P_4	P_5	P_6	P_7	P_8	P_9	P_{10}	P_L	E_c ($)	E_m (lb)
1	150.00	135.00	75.14	120.50	172.79	122.55	129.58	120.00	20.01	10.00	19.57	60798.58	4485.67
2	150.00	135.00	73.00	117.92	222.60	122.44	129.57	120.00	22.03	40.00	22.57	64487.08	4918.49
3	150.00	135.00	153.00	120.66	222.64	159.94	129.83	120.00	52.03	43.42	28.52	71950.58	5760.26
4	150.00	135.00	209.67	170.66	243.00	160.00	129.77	120.00	80.00	43.42	35.52	80147.32	7479.89
5	150.00	135.00	286.36	220.46	222.60	159.98	129.59	120.00	52.05	43.41	39.46	84063.33	9712.09
6	150.00	135.00	340.00	270.46	243.00	160.00	130.00	120.00	80.00	47.64	48.10	93405.09	12978.59
7	150.00	176.95	340.00	300.00	243.00	160.00	130.00	120.00	80.00	55.00	52.95	99401.53	14135.31
8	177.00	229.55	340.00	300.00	243.00	160.00	130.00	120.00	80.00	54.86	58.41	106426.87	14930.24
9	257.00	309.55	340.00	300.00	243.00	160.00	130.00	120.00	80.00	55.00	70.55	122936.13	17298.48
10	284.06	389.55	340.00	300.00	243.00	160.00	130.00	120.00	80.00	55.00	79.60	135865.95	20609.76
11	303.25	462.82	340.00	300.00	243.00	160.00	130.00	120.00	80.00	55.00	88.07	148255.42	28462.03
12	344.53	470.00	340.00	300.00	243.00	160.00	130.00	120.00	80.00	55.00	92.53	155284.18	30916.87
13	331.62	396.80	340.00	300.00	243.00	160.00	130.00	120.00	80.00	55.00	84.42	143039.98	22128.58
14	251.62	316.80	340.00	300.00	243.00	160.00	130.00	120.00	80.00	53.16	70.58	123104.17	17386.73
15	178.45	236.80	340.00	291.24	243.00	160.00	130.00	120.00	80.00	55.00	58.49	107011.89	14778.29
16	150.00	156.80	294.04	241.24	222.60	160.00	129.61	120.00	80.00	43.42	43.71	89056.97	10573.98
17	150.00	135.00	297.38	191.48	240.65	159.98	129.59	120.00	52.07	43.41	39.56	84053.15	9763.75
18	150.00	156.80	340.00	241.48	243.00	160.00	130.00	120.00	80.00	54.98	48.26	94201.12	12445.67
19	222.06	236.80	308.04	291.48	243.00	160.00	129.99	120.00	80.00	43.42	58.79	108008.17	14093.97
20	302.06	316.80	340.00	300.00	243.00	160.00	130.00	120.00	80.00	55.00	74.87	129078.05	18306.48
21	226.63	371.79	308.69	300.00	243.00	160.00	130.00	120.00	80.00	55.00	71.11	124899.03	17709.46
22	150.00	291.79	229.80	250.00	222.72	160.00	129.59	120.00	80.00	43.42	49.32	98973.23	10940.48
23	150.00	211.79	163.00	200.02	172.74	122.45	129.59	120.00	51.54	43.41	32.54	78934.42	6807.68
24	150.00	135.00	84.04	180.84	222.61	122.46	129.60	120.00	21.54	43.42	25.51	68144.37	5678.15
Total											1293	2471526	332301

4.1.3. Case 3: IEEE 57 Bus System (Seven Thermal Units, Three Wind Generators, and Two PV). In this case, the proposed method is used to solve a DEED on an IEEE 57 bus system. Three PV and two wind generators are incorporated into this system. The data and information of this system can be obtained from [34]. The transmission loss coefficients were taken from [24]. The predictive wind power and PV power for the 24 hours of the next day are shown in Figure 4.

The optimal load allocation scheme considering the wind and solar power unit is given in Table 10. The cost and

Table 7: Optimal results for Case 2 (optimal emission).

H	P_1	P_2	P_3	P_4	P_5	P_6	P_7	P_8	P_9	P_{10}	P_L	E_c ($)	E_m (lb)
1	150.00	135.00	90.81	91.17	129.66	129.75	97.28	97.03	80.00	55.00	19.70	63031.92	3738.78
2	150.00	137.31	101.55	101.68	144.89	144.64	108.79	108.60	80.00	55.00	22.46	66989.68	4183.90
3	165.26	165.63	120.06	120.31	171.21	160.00	129.47	120.00	80.00	55.00	28.94	75201.36	5305.11
4	200.58	201.30	145.02	145.42	205.31	160.00	130.00	120.00	80.00	55.00	36.63	85948.84	6787.74
5	218.53	218.68	158.35	158.45	221.86	160.00	130.00	120.00	80.00	55.00	40.87	90504.17	7689.93
6	254.62	255.12	190.13	190.24	243.00	160.00	130.00	120.00	80.00	55.00	50.11	102891.69	9858.75
7	274.14	274.72	210.16	210.13	243.00	160.00	130.00	120.00	80.00	55.00	55.15	109619.52	11181.43
8	292.22	292.83	231.49	231.88	243.00	160.00	130.00	120.00	80.00	55.00	60.42	115611.53	12698.72
9	325.25	325.45	278.26	278.78	243.00	160.00	130.00	120.00	80.00	55.00	71.73	128950.53	16441.33
10	348.67	348.94	316.32	300.00	243.00	160.00	130.00	120.00	80.00	55.00	79.93	138563.29	19611.66
11	382.81	383.08	340.00	300.00	243.00	160.00	130.00	120.00	80.00	55.00	87.90	148746.87	23294.05
12	407.11	407.37	340.00	300.00	243.00	160.00	130.00	120.00	80.00	55.00	92.49	156050.30	26196.89
13	364.12	364.34	340.00	300.00	243.00	160.00	130.00	120.00	80.00	55.00	84.46	144035.67	21616.38
14	325.22	325.51	278.29	278.71	243.00	160.00	130.00	120.00	80.00	55.00	71.73	128951.79	16441.32
15	292.11	292.88	231.27	232.16	243.00	160.00	130.00	120.00	80.00	55.00	60.42	115603.52	12698.75
16	232.50	233.23	170.38	182.16	235.98	160.00	130.00	120.00	80.00	55.00	45.25	95810.32	8713.92
17	218.50	218.70	158.23	158.78	221.66	160.00	130.00	120.00	80.00	55.00	40.87	90506.53	7689.94
18	254.91	255.20	189.95	190.05	243.00	160.00	130.00	120.00	80.00	55.00	50.11	102913.73	9858.75
19	291.73	292.27	231.17	233.24	243.00	160.00	130.00	120.00	80.00	55.00	60.41	115546.07	12698.93
20	338.32	338.54	299.65	283.24	243.00	160.00	130.00	120.00	80.00	55.00	75.74	133883.72	17921.35
21	345.82	346.08	257.43	259.11	243.00	160.00	130.00	120.00	80.00	55.00	72.46	132421.73	16620.31
22	265.82	266.08	177.43	209.11	214.92	160.00	130.00	120.00	80.00	55.00	50.38	104485.09	9979.33
23	185.83	186.08	119.55	159.11	170.60	160.00	128.51	120.00	80.00	55.00	32.68	81076.04	6054.37
24	150.44	150.67	110.52	110.42	157.77	157.85	118.51	118.33	80.00	55.00	25.51	70760.05	4707.21
Total											1316	2598104	291989

Table 8: Optimal compromise results for Case 2.

H	P_1	P_2	P_3	P_4	P_5	P_6	P_7	P_8	P_9	P_{10}	P_L	E_c ($)	E_m (lb)
1	150.00	135.00	83.14	105.81	122.78	122.41	93.08	120.00	79.99	43.47	19.68	61883.02	3834.71
2	150.00	135.00	93.59	118.72	129.38	127.92	123.08	120.00	80.00	54.79	22.47	65850.56	4238.58
3	150.04	135.00	151.59	130.32	174.85	160.00	129.71	120.00	80.00	55.00	28.51	72937.12	5402.22
4	151.03	165.75	176.80	180.32	222.82	160.00	130.00	120.00	80.00	55.00	35.71	81513.33	7057.05
5	150.77	214.81	185.63	180.84	243.00	160.00	130.00	120.00	80.00	55.00	40.05	86940.85	7951.01
6	225.74	222.30	210.98	230.26	243.00	159.98	130.00	120.00	80.00	55.00	49.27	98933.28	10070.42
7	226.84	224.58	274.93	241.60	243.00	159.95	130.00	120.00	80.00	55.00	53.89	103218.06	11766.89
8	227.09	245.31	287.77	286.75	243.00	160.00	130.00	120.00	80.00	55.00	58.92	109001.40	13533.34
9	298.28	309.59	299.19	300.00	243.00	160.00	130.00	120.00	80.00	55.00	71.06	125030.20	16622.95
10	327.06	346.48	340.00	300.00	243.00	160.00	130.00	120.00	80.00	55.00	79.55	136668.76	19755.86
11	377.53	388.34	340.00	300.00	243.00	160.00	130.00	120.00	80.00	55.00	87.88	148487.46	23312.06
12	393.65	420.79	340.00	300.00	243.00	160.00	130.00	120.00	80.00	55.00	92.45	155752.75	26388.10
13	352.11	376.30	340.00	300.00	243.00	160.00	130.00	120.00	80.00	55.00	84.43	143741.53	21683.51
14	298.74	309.52	298.81	300.00	243.00	160.00	130.00	120.00	80.00	55.00	71.07	125046.92	16619.27
15	230.58	282.70	276.52	257.58	243.00	160.00	130.00	120.00	80.00	55.00	59.39	111102.30	13124.72
16	150.58	215.75	202.69	241.08	243.00	160.00	130.00	120.00	79.99	55.00	44.10	91219.05	9331.48
17	150.05	142.50	198.41	240.44	243.00	160.00	130.00	120.00	80.00	55.00	39.41	84745.32	8567.45
18	164.97	222.36	259.72	241.58	243.00	160.00	130.00	120.00	80.00	55.00	48.63	96388.38	10708.27
19	234.65	244.68	286.27	281.39	243.00	160.00	130.00	120.00	80.00	55.00	59.00	109550.71	13431.70
20	307.82	320.50	330.66	300.00	243.00	160.00	130.00	120.00	80.00	55.00	74.99	129799.15	18164.80
21	303.25	348.25	265.30	290.89	243.00	160.00	130.00	120.00	80.00	55.00	71.71	128557.39	16591.91
22	223.25	268.25	185.39	240.89	222.65	160.00	129.62	120.00	80.00	47.70	49.76	100925.52	10228.10
23	150.00	188.25	129.33	190.89	172.74	160.00	129.60	120.00	80.00	43.43	32.24	78684.55	6327.54
24	150.00	135.00	98.73	140.89	172.61	139.05	129.56	120.00	79.99	43.55	25.37	68907.17	4873.13
Total											1300	2514885	299585

emission are 111203.2 $/day and 115221.2 lb/day, respectively. MODE and NSGA-II were used for comparison. It can be seen that the proposed method has better performance both in cost and emission. Moreover, we studied the impact of the introduction of RES on the system. Figure 5 shows that both cost and emission have improved.

Table 9: Comparison with MODE and NSGA-II for Case 2.

Method	Minimum cost				Minimum emission			
	Minimum cost ($)	Mean cost ($)	Maximum cost ($)	Standard deviation	Minimum emission (lb)	Mean emission (lb)	Maximum emission (lb)	Standard deviation
NSGA-II	2520648	2521741	2522085	1307	298464	299157	300146	237
MODE	2512327	2515319	2519422	1876	296453	297150	298607	423
SHHA	2471526	2473890	2478533	757	291988	292013	292475	157

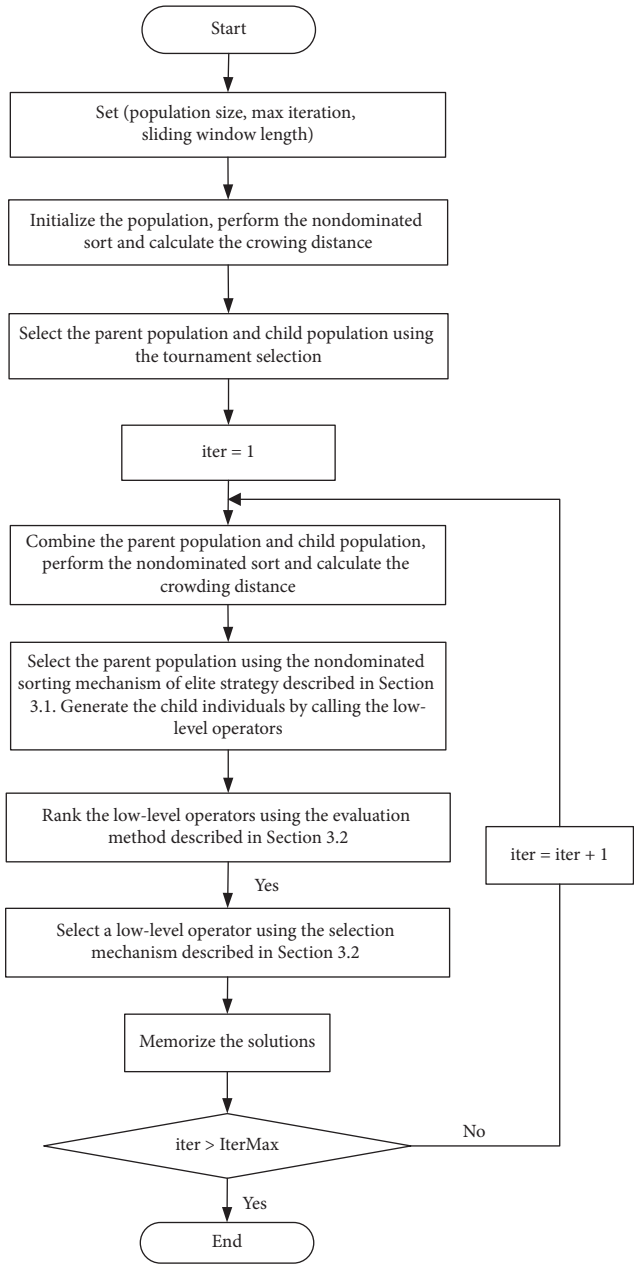

Figure 2: Flowchart of the proposed SHHA for DEED.

The cost and emission before introducing wind power and PV generators are 119305.6 $/day and 127416.7 lb/day, which means the introduction of RES will save about 8102.4 $ per day (approximately 2,957,376 $ per year) and reduce emissions 12195.5 lb per day (approximately 4,451,357 lb per year) (Table 11).

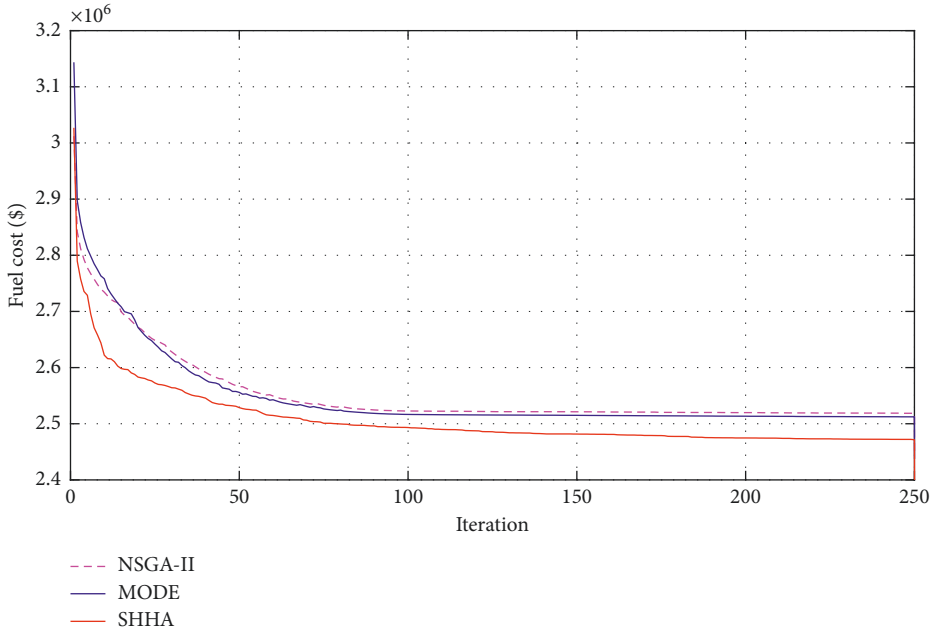

Figure 3: Convergence graphs of NSGA-II, MODE, and SHHA.

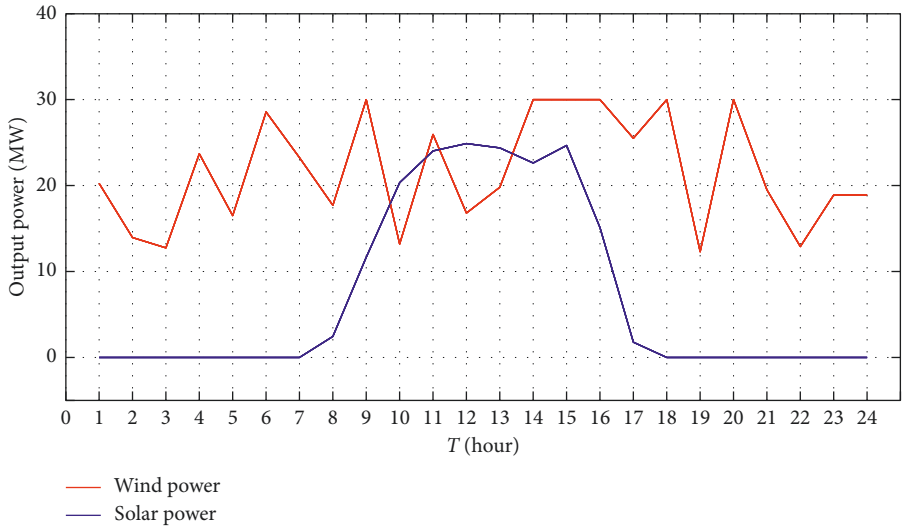

Figure 4: Predictive wind power and solar power for the 24 hours, next day t.

4.1.4. Case 4: Case 3 with Energy Storage. In this case, the ES unit is considered on the basis of Case 3. Relevant parameters of thermal units, wind power generators, PV generators, and transmission loss coefficient are consistent with Case 3. Parameters of ES can be found in Table 1. The initial value of SOC is set to 0.5, and the SOC at each hour can be accessed by

$$\begin{aligned} \mathrm{SOC}_i(t+1) &= \mathrm{SOC}_i(t) - \frac{\eta_c \mathrm{ES}_{i,t} \Delta t}{E \max}, \quad \mathrm{ES}_{i,t} < 0, \\ \mathrm{SOC}_i(t+1) &= \mathrm{SOC}_i(t) - \frac{\mathrm{ES}_{i,t}(\Delta t/\eta_d)}{E \max}, \quad \mathrm{ES}_{i,t} > 0, \end{aligned} \tag{20}$$

where η_c is the charge efficiency, η_d is the discharge efficiency, and $E_{\max}$ is the ES energy capacity. Table 12 lists the optimal compromise solution. The optimal compromise solution corresponding to the cost is 111317.6 $/day and the emission is 14565.4 lb/day. At the beginning of the day, the power load is in the low stage, at which time the power demand is less and the ES is in charge mode to store energy for future peak shaving. It is assumed that the initial SOC is 0.5 and the total charge power per hour should meet the upper limit. In the peak load stage, the ES is in the discharge mode to reduce the power generation of the grid. Finally, the ES state will be restored to 0.5 SOC at the end of the day. Figure 6 shows the effect of ES on load peak shaving and valley filling. Figure 6 reflects the impact of the introduction of ES on the Pareto optimal solution set. It can be seen that ES is beneficial to both cost and emission (Figure 7).

Table 10: Optimal compromise results for Case 3.

H	P_1	P_2	P_3	P_4	P_5	P_6	P_7	P_{w1}	P_{w2}	P_{w3}	P_{v1}	P_{v2}	P_L	E_c ($)	E_m (lb)
1	207.88	10.00	20.00	10.13	211.59	10.00	133.89	20.25	20.25	20.25	0.00	0.00	28.22	1722.8	1136.3
2	238.85	10.00	20.00	10.01	244.37	10.00	162.03	13.95	13.95	13.95	0.00	0.00	27.19	1970.3	1561.3
3	279.80	10.00	37.58	10.00	284.31	10.23	219.74	12.75	12.75	12.75	0.00	0.00	31.93	2516.1	2349.5
4	304.15	10.00	59.53	14.39	331.87	11.53	246.27	23.70	23.70	23.70	0.00	0.00	42.80	3050.7	3067.4
5	334.69	10.00	64.90	25.97	346.52	25.01	265.61	16.50	16.50	16.50	0.00	0.00	42.21	3552.5	3572.3
6	350.87	10.00	87.43	36.21	380.16	37.74	296.46	28.56	28.56	28.56	0.00	0.00	56.52	4252.1	4327.5
7	368.85	10.00	88.43	46.29	399.99	54.77	319.05	23.25	23.25	23.25	0.00	0.00	55.19	4762.5	4910.6
8	383.13	10.00	105.47	61.15	428.97	57.41	327.55	17.70	17.70	17.70	2.45	2.45	55.71	5272.2	5506.9
9	401.92	10.00	120.06	75.48	457.63	66.99	355.61	30.00	30.00	30.00	11.66	11.66	77.02	5941.2	6387.6
10	418.77	10.00	126.24	80.87	481.89	90.01	388.38	23.24	28.39	13.20	20.33	20.33	79.65	6862.5	7296.9
11	440.30	10.00	133.99	93.99	501.18	97.35	396.75	25.95	25.95	25.95	24.03	24.03	93.44	7088.3	7954.9
12	459.87	10.00	140.00	100.00	520.44	100.00	410.00	16.80	16.81	16.80	24.88	24.88	90.59	7436.2	8625.0
13	435.72	10.00	135.06	95.59	493.95	88.81	391.27	19.80	19.80	19.80	24.38	24.38	86.56	6950.3	7735.7
14	403.63	10.00	111.03	68.33	443.94	75.62	361.05	30.00	30.00	30.00	22.62	22.62	84.85	5859.9	6269.7
15	363.52	10.00	95.44	53.02	417.99	52.94	320.31	30.00	30.00	30.00	24.66	24.66	76.56	4922.9	5093.0
16	330.46	10.00	69.90	26.19	350.08	28.12	279.02	30.00	30.00	30.00	15.11	15.11	60.01	3679.4	3687.2
17	320.59	10.00	64.76	15.07	341.61	23.47	261.00	25.50	25.50	25.50	13.17	1.78	47.94	3469.3	3383.8
18	347.91	10.00	73.77	37.41	388.39	46.65	290.09	30.00	30.00	30.00	0.00	0.00	56.18	4240.5	4306.7
19	382.46	10.00	101.22	52.52	423.75	59.35	327.42	30.00	30.00	20.90	0.00	0.00	61.71	5521.6	5413.1
20	416.53	10.00	122.12	79.00	469.79	82.42	377.39	30.00	30.00	30.00	0.00	0.00	75.27	6355.6	6959.6
21	413.07	10.00	130.99	76.35	463.05	71.49	365.92	19.50	19.50	19.50	0.00	0.00	65.44	6196.3	6726.0
22	357.03	10.00	88.89	45.99	387.16	46.49	296.83	13.88	15.35	12.90	0.00	0.00	46.51	4537.3	4481.3
23	286.36	10.00	54.33	10.00	303.20	21.49	226.77	18.90	18.90	18.90	0.00	0.00	36.88	2862.5	2598.8
24	257.14	10.00	24.54	10.00	259.24	10.00	188.25	18.90	18.90	18.90	0.00	0.00	31.93	2180.4	1870.0
Total													1410	111203	115221

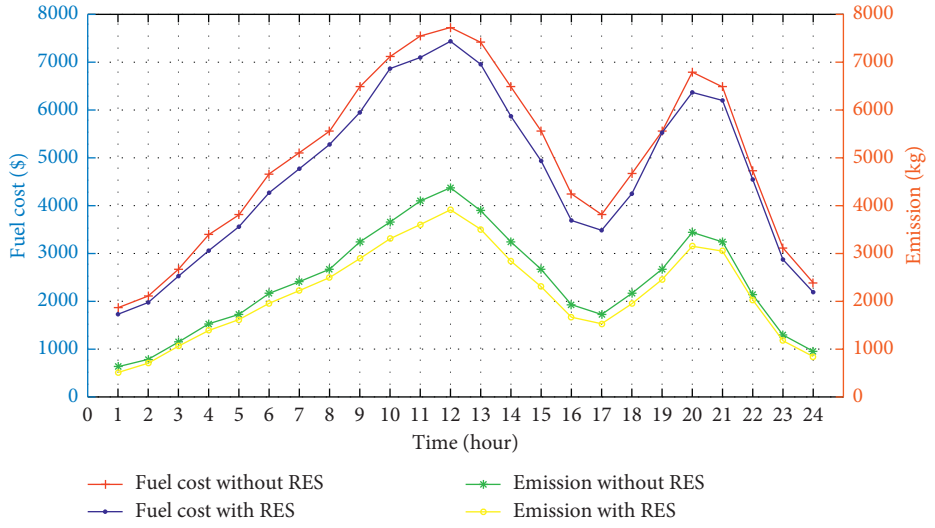

Figure 5: The impact of PV and wind power generation on cost and emission.

Table 11: Comparison with MODE and NSGA-II.

Method	Compromise result	
	E_c ($)	E_m (lb)
MODE	115067	118513
NSGA-II	113847	115854
With RES (this paper)	111203	115221

4.2. Effect of High-Level Strategy. In the hyper-heuristic method, the high-level strategy is used to evaluate each low-level operator and then determine the chosen probability of each operator for the following searching iterations. Figure 8 shows the change of the chosen probability of each low-level operator and it can be seen that the operators are adapting to the whole iteration. The operators show a significant difference in chosen probability at different iterations, which means that they have a different searching performance at different stages of the evolution process. Here, we only discuss the role of high-level strategy, without regard to the effect of the parameter setting of low-level operators.

Table 12: Optimal compromise results for Case 4.

H	P_1	P_2	P_3	P_4	P_5	P_6	P_7	P_{w1}	P_{w2}	P_{w3}	P_{v1}	P_{v2}	ES	P_L	E_c ($)	E_m (lb)
1	210.58	10.00	20.90	10.00	239.23	16.59	148.29	20.25	20.25	20.25	0.00	0.00	−51.84	28.48	1919.73	1346.75
2	227.56	10.00	23.66	10.08	285.41	12.60	169.08	13.95	13.95	13.95	0.00	0.00	−43.85	26.40	2132.58	1796.30
3	268.86	10.00	39.37	13.95	293.68	36.57	219.14	12.75	12.75	12.75	0.00	0.00	−30.80	31.02	2841.36	2372.17
4	329.83	10.00	62.87	15.25	323.36	13.60	246.87	23.70	23.70	23.70	0.00	0.00	−20.88	46.01	3156.58	3194.41
5	324.13	10.06	72.78	23.25	345.15	38.60	271.18	16.50	16.50	16.50	0.00	0.00	−12.65	42.00	3719.48	3557.49
6	361.42	10.18	82.90	41.83	366.08	40.23	300.99	28.56	28.56	28.56	0.00	0.00	−3.02	58.28	4307.78	4319.56
7	372.49	10.00	97.98	41.66	399.17	48.63	313.33	23.25	23.25	23.25	0.00	0.00	5.26	56.27	4710.99	4894.39
8	388.33	10.16	96.26	63.62	421.02	51.54	329.52	17.70	17.70	17.70	2.45	2.45	13.50	55.96	5154.90	5446.31
9	403.47	10.02	119.39	52.14	451.51	73.59	354.87	30.00	30.00	30.00	11.66	11.66	22.39	76.71	5728.31	6280.64
10	398.89	10.00	122.71	80.82	489.11	86.33	371.36	23.24	28.39	13.20	20.33	20.33	32.56	75.28	6678.22	6984.72
11	436.48	10.02	136.19	94.10	463.90	97.06	396.79	25.95	25.95	25.95	24.03	24.03	38.66	93.11	6962.08	7475.63
12	460.44	10.00	138.15	98.88	520.67	97.33	367.71	16.80	16.81	16.80	24.88	24.88	45.36	88.71	7194.52	8141.38
13	434.34	10.00	106.95	96.23	480.78	95.11	386.01	19.80	19.80	19.80	24.38	24.38	37.10	82.67	6709.36	7402.29
14	399.84	10.01	116.52	50.93	444.04	71.10	360.40	30.00	30.00	30.00	22.62	22.62	20.29	84.39	5647.54	6197.23
15	367.02	10.34	100.54	46.35	410.98	49.86	324.18	30.00	30.00	30.00	24.66	24.66	5.69	78.27	4865.17	5083.80
16	328.66	10.00	75.10	66.49	357.86	34.55	302.90	30.00	30.00	30.00	15.11	15.11	−80.00	61.78	4341.00	4030.14
17	306.08	10.01	78.12	23.07	405.77	30.02	262.76	25.50	25.50	25.50	13.17	1.78	−80.00	47.27	3898.79	3931.54
18	354.33	10.05	113.64	49.75	376.57	41.42	335.07	30.00	30.00	30.00	0.00	0.00	−80.00	62.82	4814.52	4788.80
19	339.83	10.00	99.48	54.99	421.26	60.38	324.08	30.00	30.00	20.90	0.00	0.00	40.76	55.69	5397.64	5008.34
20	400.81	10.01	130.39	45.46	464.70	60.33	362.39	30.00	30.00	30.00	0.00	0.00	80.00	72.08	5669.78	6485.53
21	405.26	10.00	93.05	81.18	462.29	41.22	351.87	19.50	19.50	19.50	0.00	0.00	80.00	59.37	5498.55	6290.76
22	353.10	10.21	85.54	46.98	387.28	47.03	299.69	13.88	15.35	12.90	0.00	0.00	2.38	46.34	4528.08	4466.87
23	285.78	10.32	54.28	10.36	301.81	22.10	269.04	18.90	18.90	18.90	0.00	0.00	−39.29	39.10	3023.24	2872.09
24	306.56	10.00	36.01	10.21	261.75	11.13	187.17	18.90	18.90	18.90	0.00	0.00	−58.54	37.00	2417.43	2198.29
Total														1405	111318	114565

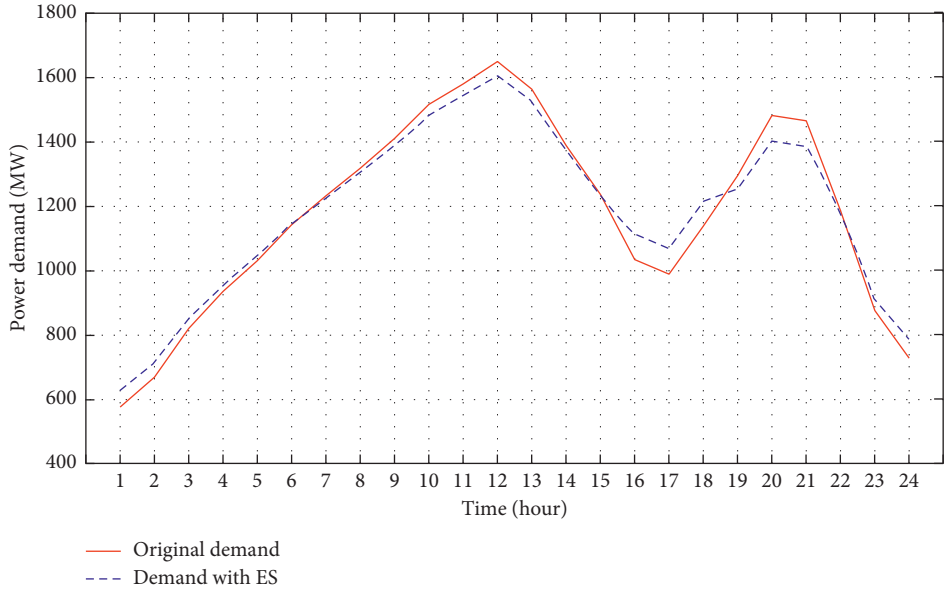

Figure 6: Effect of ES on load demand.

4.3. Effect of Elitist Nondominated Sorting Strategy. Population diversity is an important indicator to evaluate convergence and search performance of algorithms, especially in dealing with optimization problems with nonlinear and multipeak characteristics. To demonstrate the effectiveness of the proposed nondominated sorting strategy, we recorded the results of individual selection with and without the elite sorting strategy. Figure 9 shows the comparison results, where the red points represent the distribution of individuals screened by using the elite strategy. We can find from the figure that the population has better performance in individual distribution. The elite strategy effectively keeps the population diversity.

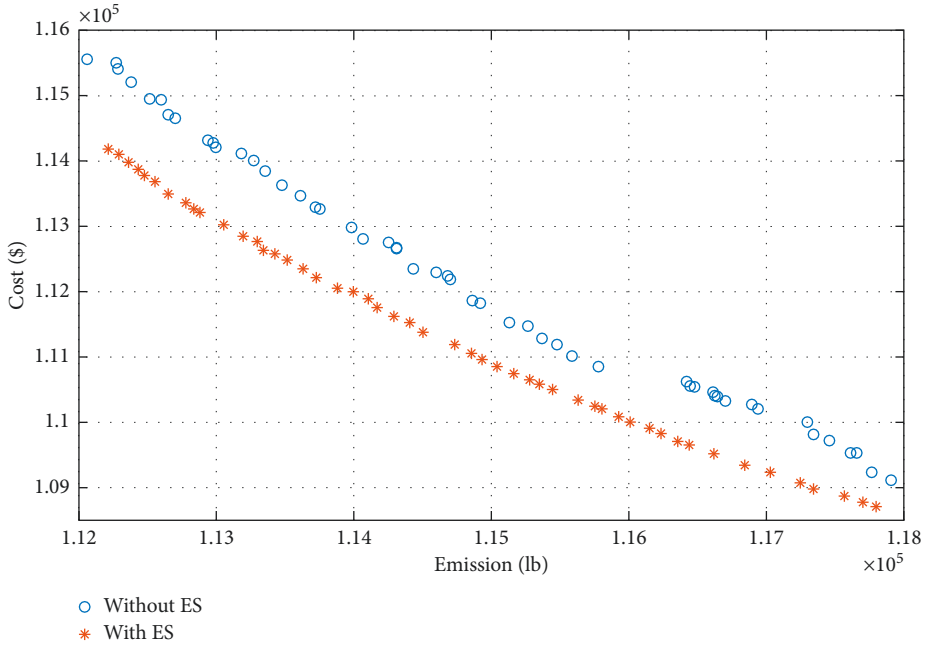

Figure 7: Effect of ES on load demand.

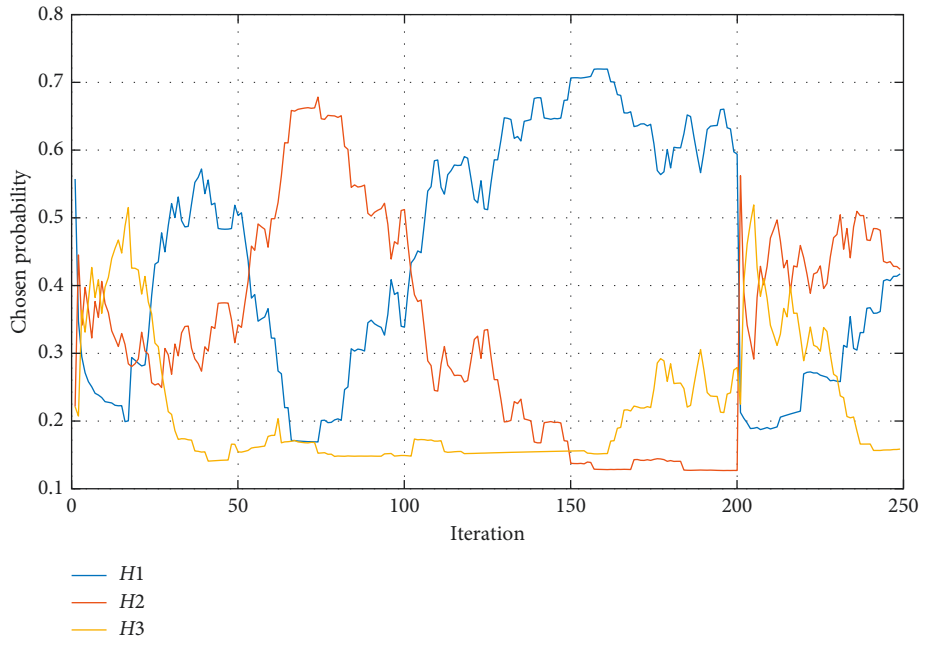

Figure 8: Chosen probability of low-level operators.

4.4. Effect of Constraint Handling. Constraint handling presented in Section 3 aims to transform the infeasible individuals into high-quality feasible individuals. To demonstrate its effectiveness, we record the average cost with and without the handling procedure in the same experiment situation. A constraint handling method in [35] is used for comparison, and we have further improved it on the basis of this method. The difference in power demand Dif is no longer added directly to the adjusted operator but multiplied with a random factor Δ. This will make the adjustment of power balance constraints more balanced without losing the characteristics of random allocation. Table 13 shows that each case with the proposed constraint handling can find a better solution. When a feasible solution P_t is obtained at the current hour, it may make it impossible for P_{t+1} to meet the power balance and ramp rate constraints at the next hour. Failure times refer to the number of times of the situation that the constraints cannot be met. Lower failure times mean an effective

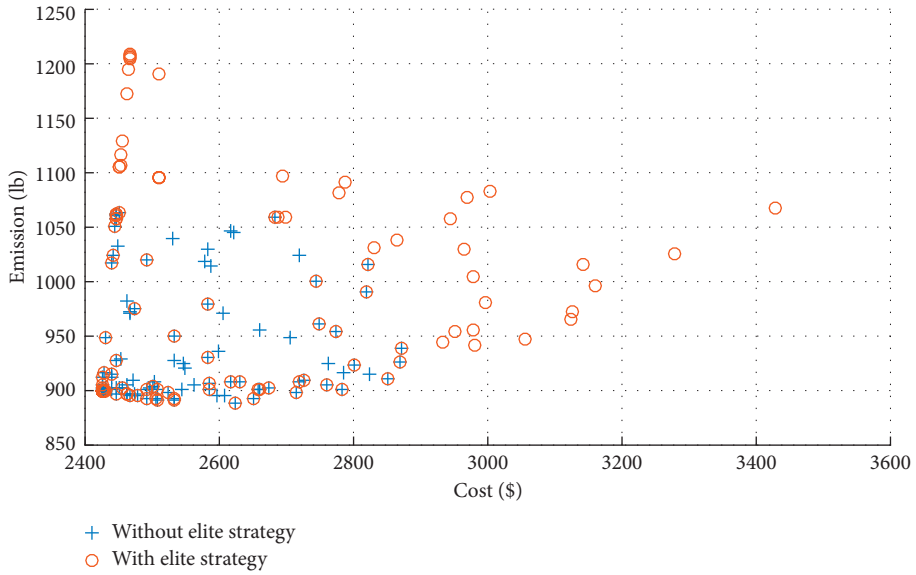

Figure 9: Impact of the elitist nondominated sorting strategy on individual screening.

Table 13: Comparison with and without the proposed constraint handling method.

System	Cost saving		Reduction percentage (%)
	E_c ($)/day	E_m (lb)/day	
Case 1	182	55	15
Case 2	412	177	19
Case 3	367	286	19
Case 4	201	137	12

constraint-handling strategy. We record the reduction percentage in the number of failures. It can be seen from Table 12 that the cost and emission are all improved and the number of failure times has been further reduced.

5. Conclusions

Building a low-carbon future has been an important and urgent task under Paris Global Agreement. Dynamic economic emission dispatch has long been a complex problem which aims to effectively save the fossil fuel cost, relief energy waste, and reduce environmental pollution. Moreover, as renewable energy is considered, the complexity of the DEED is further enhanced. In this paper, a mathematical model of the multiobjective dynamic economic and environmental load distribution problem including wind energy, solar power generation units, and ES is established. A multiobjective hyper-heuristic algorithm is proposed to solve the problem. Four test cases in 24-hour time period are tested to verify the effectiveness of the proposed algorithm.

The main contributions of this study can be summarized as follows: (1) we provide a new way of solving such coupled spatial-temporal scheduling problems in the power system. The hyper-heuristic algorithm is used to solve multiobjective DEED problems. Researchers can replace the low-level operators of our algorithm with their own methods to further improve the search capability. (2) For improving search capability and diversity distribution of Pareto front, an elitist nondominated sorting strategy is adopted to guide the screen of parent individuals. (3) An effective strategy is introduced to transform infeasible solutions towards feasible ones to enhance the quality of solutions and the convergence rate of the proposed algorithm.

In future work, we plan to further study the high level of the hyper-heuristics. The proposed algorithm is a selection hyper-heuristic algorithm, in which the low-level operators need to be pregiven. Further work will explore the generation hyper-heuristics to automatically designed operators. On the other hand, a renewable energy source such as electric vehicles will be integrated into the system dispatch to comprehensively study the power system.

Data Availability

The authors pledge to provide all the codes and the data underlying the findings of the study.

Conflicts of Interest

The authors declare that there are no conflicts of interest regarding the publication of this paper.

Acknowledgments

The authors would like to thank the National Natural Science Foundation of China (grant nos. 61773105, 61533007,

61873049, 61873053, 61703085, and 61374147) and the Fundamental Research Funds for the Central Universities (grant no. N182008004) for supporting this research work.

References

[1] Z. Yang, K. Li, Q. Niu, Y. Xue, and A. Foley, "A self-learning TLBO based dynamic economic/environmental dispatch considering multiple plug-in electric vehicle loads," *Journal of Modern Power Systems and Clean Energy*, vol. 2, no. 4, pp. 298–307, 2014.

[2] T. Cheng, M. Chen, and Y. Wang, "Adaptive robust method for dynamic economic emission dispatch incorporating renewable energy and energy storage," *Complexity*, vol. 2018, Article ID 2517987, 13 pages, 2018.

[3] C. Wei, L. Qu, and W. Qiao, "Evaluation of ANN estimation-based MPPT control for a DFIG wind turbine," in *Proceedings of the 2014 IEEE Symposium on Power Electronics and MDachines for Wind and Water Applications*, Milwaukee WI, USA, July 2014.

[4] X. Bai, W. Qiao, H. Wei, F. Huang, and Y. Chen, "Bidirectional coordinating dispatch of large-scale V2G in a future smart grid using complementarity optimization," *International Journal of Electrical Power & Energy Systems*, vol. 68, pp. 269–277, 2015.

[5] Y. Zhang, F. Yao, H. H.-C. Iu, T. Fernando, and K. P. Wong, "Sequential quadratic programming particle swarm optimization for wind power system operations considering emissions," *Journal of Modern Power Systems and Clean Energy*, vol. 1, no. 3, pp. 231–240, 2013.

[6] N. Pandit, A. Tripathi, S. Tapaswi, and M. Pandit, "An improved bacterial foraging algorithm for combined static/dynamic environmental economic dispatch," *Applied Soft Computing*, vol. 12, no. 11, pp. 3500–3513, 2012.

[7] N. A. Khan, A. B. Awan, A. Mahmood, S. Razzaq, A. Zafar, and G. A. S. Sidhu, "Combined emission economic dispatch of power system including solar photo voltaic generation," *Energy Conversion and Management*, vol. 92, pp. 82–91, 2015.

[8] Z. Hu, M. Zhang, X. Wang, C. Li, and M. Hu, "Bi-level robust dynamic economic emission dispatch considering wind power uncertainty," *Electric Power Systems Research*, vol. 135, pp. 35–47, 2016.

[9] J. Jin, D. Zhou, P. Zhou, S. Qian, and M. Zhang, "Dispatching strategies for coordinating environmental awareness and risk perception in wind power integrated system," *Energy*, vol. 106, pp. 453–463, 2016.

[10] J. Zhou, P. Lu, Y. Li, C. Wang, L. Yuan, and L. Mo, "Short-term hydro-thermal-wind complementary scheduling considering uncertainty of wind power using an enhanced multi-objective bee colony optimization algorithm," *Energy Conversion and Management*, vol. 123, pp. 116–129, 2016.

[11] F. Zaman, S. M. Elsayed, T. Ray, and R. A. Sarker, "Configuring two-algorithm-based evolutionary approach for solving dynamic economic dispatch problems," *Engineering Applications of Artificial Intelligence*, vol. 53, pp. 105–125, 2016.

[12] M. Nazari-Heris, B. Mohammadi-Ivatloo, and G. B. Gharehpetian, "A comprehensive review of heuristic optimization algorithms for optimal combined heat and power dispatch from economic and environmental perspectives," *Renewable and Sustainable Energy Reviews*, vol. 81, pp. 2128–2143, 2018.

[13] Z. Yang, K. Li, Q. Niu, and Y. Xue, "A comprehensive study of economic unit commitment of power systems integrating various renewable generations and plug-in electric vehicles," *Energy Conversion and Management*, vol. 132, pp. 460–481, 2017.

[14] G. Liu, Y. L. Zhu, and W. Jiang, "Wind-thermal dynamic economic emission dispatch with a hybrid multi-objective algorithm based on wind speed statistical analysis," *IET Generation, Transmission & Distribution*, vol. 12, no. 17, pp. 3972–3984, 2018.

[15] R. Bai, J. Blazewicz, E. K. Burke, G. Kendall, and B. McCollum, "A simulated annealing hyper-heuristic methodology for flexible decision support," *4OR*, vol. 10, no. 1, pp. 43–66, 2012.

[16] E. K. Burke, "A classification of hyper-heuristic approaches," in *Handbook of Metaheuristics*, M. Gendreau and J.-Y. Potvin, Eds., pp. 449–468, Springer, Boston, MA, USA, 2010.

[17] K. Deb, A. Pratap, S. Agarwal, and T. Meyarivan, "A fast and elitist multiobjective genetic algorithm: NSGA-II," *IEEE Transactions on Evolutionary Computation*, vol. 6, no. 2, pp. 182–197, 2002.

[18] Y. Zhang, D.-W. Gong, N. Geng, and X.-Y. Sun, "Hybrid bare-bones PSO for dynamic economic dispatch with valve-point effects," *Applied Soft Computing*, vol. 18, pp. 248–260, 2014.

[19] T. Niknam, R. Azizipanah-Abarghooee, M. Zare, and B. Bahmani-Firouzi, "Reserve constrained dynamic environmental/economic dispatch: a new multiobjective self-adaptive learning bat algorithm," *IEEE Systems Journal*, vol. 7, no. 4, pp. 763–776, 2013.

[20] W. Mingqiang, H. B. Gooi, S. Chen, and S. Lu, "A mixed integer quadratic programming for dynamic economic dispatch with valve point effect," in *Proceedings of the 2015 IEEE Power & Energy Society General Meeting*, Denver, CO, USA, July 2015.

[21] W. Center, *Wind and Solar Power Systems*, CRC Press, Boca Raton, FL, USA, 1999.

[22] J. Hetzer, D. C. Yu, and K. Bhattarai, "An economic dispatch model incorporating wind power," *IEEE Transactions on Energy Conversion*, vol. 23, no. 2, pp. 603–611, 2008.

[23] J. Zeng and W. Qiao, "Short-term solar power prediction using an RBF neural network," in *Proceedings of the 2011 IEEE Power and Energy Society General Meeting*, Detroit, MI, USA, July 2011.

[24] G. Mohy-ud-din, "Hybrid dynamic economic emission dispatch of thermal, wind, and photovoltaic power using the hybrid backtracking search algorithm with sequential quadratic programming," *Journal of Renewable and Sustainable Energy*, vol. 9, no. 1, Article ID 015502, 2017.

[25] C. K. Panigrahi, P. K. Chattopadhyay, R. N. Chakrabarti, and M. Basu, "Simulated annealing technique for dynamic economic dispatch," *Electric Power Components and Systems*, vol. 34, no. 5, pp. 577–586, 2006.

[26] M. Basu, "Dynamic economic emission dispatch using nondominated sorting genetic algorithm-II," *International Journal of Electrical Power & Energy Systems*, vol. 30, no. 2, pp. 140–149, 2008.

[27] S. Hemamalini and S. P. Simon, "Dynamic economic dispatch using Maclaurin series based Lagrangian method," *Energy Conversion and Management*, vol. 51, no. 11, pp. 2212–2219, 2010.

[28] J. S. Alsumait, M. Qasem, J. K. Sykulski, and A. K. Al-Othman, "An improved pattern search based algorithm to solve the dynamic economic dispatch problem with valve-point effect," *Energy Conversion and Management*, vol. 51, no. 10, pp. 2062–2067, 2010.

[29] M. Basu, "Dynamic economic emission dispatch using evolutionary programming and fuzzy satisfying method,"

International Journal of Emerging Electric Power Systems, vol. 8, no. 4, 2007.

[30] H. Zhang, "Adaptive grid based multi-objective Cauchy differential evolution for stochastic dynamic economic emission dispatch with wind power uncertainty," *PLoS One*, vol. 12, no. 9, Article ID e0185454, 2017.

[31] H. Zhang, D. Yue, X. Xie, S. Hu, and S. Weng, "Multi-elite guide hybrid differential evolution with simulated annealing technique for dynamic economic emission dispatch," *Applied Soft Computing*, vol. 34, pp. 312–323, 2015.

[32] P. Attaviriyanupap, H. Kita, E. Tanaka, and J. Hasegawa, "A hybrid EP and SQP for dynamic economic dispatch with nonsmooth fuel cost function," *IEEE Transactions on Power Systems*, vol. 17, no. 2, pp. 411–416, 2002.

[33] L. Xuebin, "Study of multi-objective optimization and multi-attribute decision-making for dynamic economic emission dispatch," *Electric Power Components and Systems*, vol. 37, no. 10, pp. 1133–1148, 2009.

[34] P. Karthikeyan, "Security constrained unit commitment problem with operational Power flow and environmental constraints," *WSEAS Transactions on Power Systems*, vol. 4, pp. 53–56, 2009.

[35] D. He, L. Yang, X. Tian, and Z. Wang, "An overlapped decomposition optimization method for dynamic economic dispatch," *IEEE Access*, vol. 6, pp. 45804–45820, 2018.

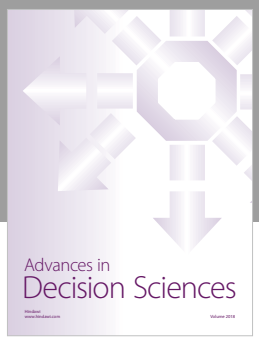

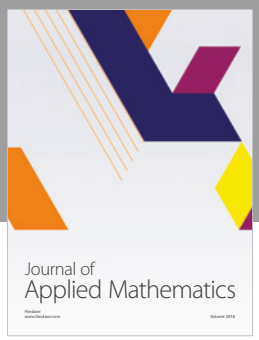

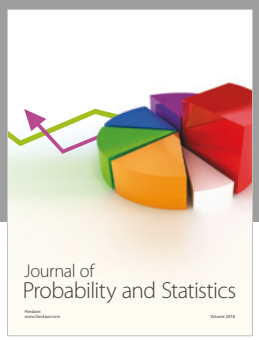

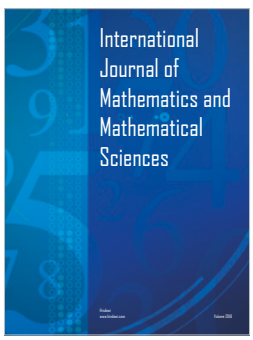

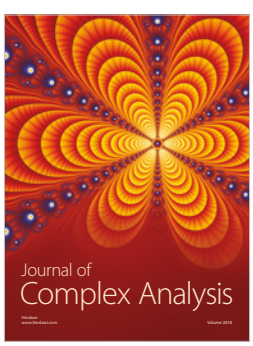

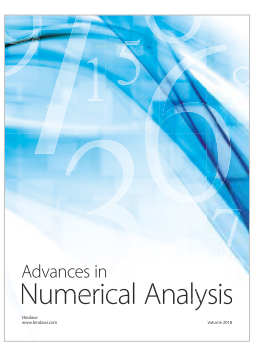

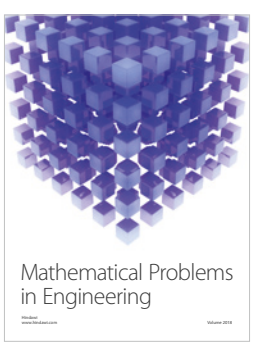

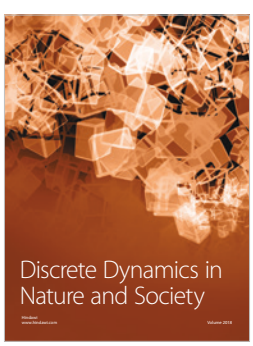

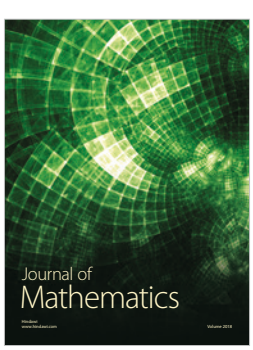

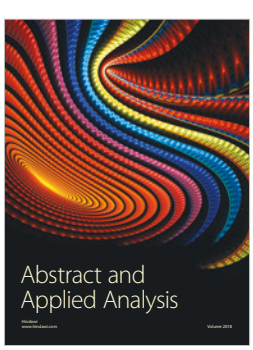

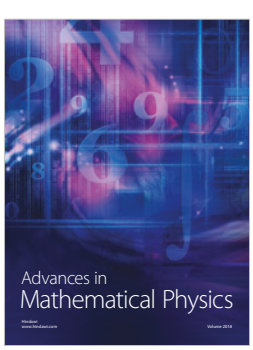

Hindawi

Submit your manuscripts at
www.hindawi.com